Longitudinal ionospheric effects in the South Atlantic evening sector during solar maximum

E. R. de Paula,[1] J. R. Souza,[1] B. G. Fejer,[2] G. J. Bailey,[3] and R. A. Heelis[4]

Received 11 September 2001; revised 10 December 2001; accepted 11 December 2001; published 10 July 2002.

[1] Large-scale horizontal gradients in ion density and vertical drift observed by the Atmospheric Explorer E satellite in the South Atlantic region (latitudes 10°S–20°S, longitudes 50°W–10°E) during the June solstice at solar maximum are presented and analyzed. These features occur during the nighttime period. The observations near 450-km altitude show vertically downward ion drift velocities exceeding 120 m s^{-1} and depleted regions where the ion density is around 2×10^4 cm^{-3}. It is shown, using values modeled by the Sheffield University Plasmasphere Ionosphere Model (SUPIM) along the satellite trajectory, that the large ion density depletions appear as a result of large downward ion drifts driven by large southward winds along the magnetic meridian and by diffusion. During others seasons such behavior is not observed by the AE-E satellite, neither by SUPIM results. The roles played by the different physical processes responsible for the large downward drift velocities are investigated. The model results highlight the relationship between longitudinal variation of the ion densities and the location of the equatorial anomaly crest in the South Atlantic region. *INDEX TERMS:* 2415 Ionosphere: Equatorial ionosphere; 2437 Ionosphere: Ionospheric dynamics; 2447 Ionosphere: Modeling and forecasting; *KEYWORDS:* equatorial ionosphere, vertical plasma drifts, meridional wind, ionic density, ionospheric modeling

1. Introduction

[2] The occurrence of large longitudinal variations in the quiet time low-latitude evening and nighttime ionosphere has been known for several decades. These longitudinal variations are particularly large in the American-African sector, where they are evident, for example, in the vertical ion drift velocity, strength of the Appleton anomaly, and the occurrence of equatorial spread *F* [e.g., *Batista et al.*, 1986; *Fejer et al.*, 1991, 1993, 1995; *Abdu et al.*, 1998]. They have been attributed to the displacement of the geographic and geomagnetic equators, and the longitudinal variations of the strength and declination of the geomagnetic field. Recently, ground-based and satellite studies have shown strong longitudinal variations in the occurrence of low-latitude *F* region plasma irregularities and topside ion densities in the American sector also during periods of large geomagnetic disturbances [*Basu et al.*, 2001; *Sultan et al.*, 2001]. These effects have also been attributed to longitudinal changes in the equatorial disturbance electric field.

[3] Model studies indicate that the longitudinal variation of the equatorial vertical electrodynamic ($\mathbf{E} \times \mathbf{B}$) drift produces large changes in the evening and nighttime equatorial *F* region plasma densities [e.g., Anderson et al., 1973]. *Dachev and Walker* [1982] have studied large-scale low-altitude (250–320 km) nocturnal plasma depletions in the low-latitude *F* region using in situ observations by the Atmospheric Explorer-C (AE–C) and Atmospheric Explorer-E (AE-E) satellites. These depletions are most developed in the premidnight sector and occur in the summer hemisphere regions of large magnetic declination during the solstices and near the magnetic equator during equinox. *Dachev and Walker* [1982] explained their occurrence as due to the upward ion drift velocity, which raises the *F* region above the altitude of the satellite. These authors also reported AE-E observations of a region of large nighttime plasma depletion during June solstice months between 50°W–10°E and 10°S–20°S at an altitude of ~450 km and suggested that the depletion could be due to large downward ion drift velocities. It is interesting to note that several recent studies have reported unusual ionospheric morphology near the South Atlantic magnetic anomaly region where the strength of the geomagnetic field is small and the magnetic declination is large [*Venkatraman and Heelis*, 1999; *Souza et al.*, 2000a, 2000b].

[4] In this paper, we initially present simultaneous observations of large ion density depletions and vertical ion drift velocities measured by the AE-E satellite as it passes through the South American-African region. These vertical drift measurements were not available to Dachev and Walker. Then, we present values obtained from numerical simulations using the Sheffield University Plasmasphere

[1]Instituto Nacional de Pesquisas Espaciais, São José dos Campos, São Paulo, Brazil.
[2]Center for Atmospheric and Space Sciences, Utah State University, Logan, Utah, USA.
[3]Department of Applied Mathematics, University of Sheffield, Sheffield, England, UK.
[4]W. B. Hanson Center for Space Sciences, University of Texas at Dallas, Richardson, Texas, USA.

0148-0227/02/2001JA000298

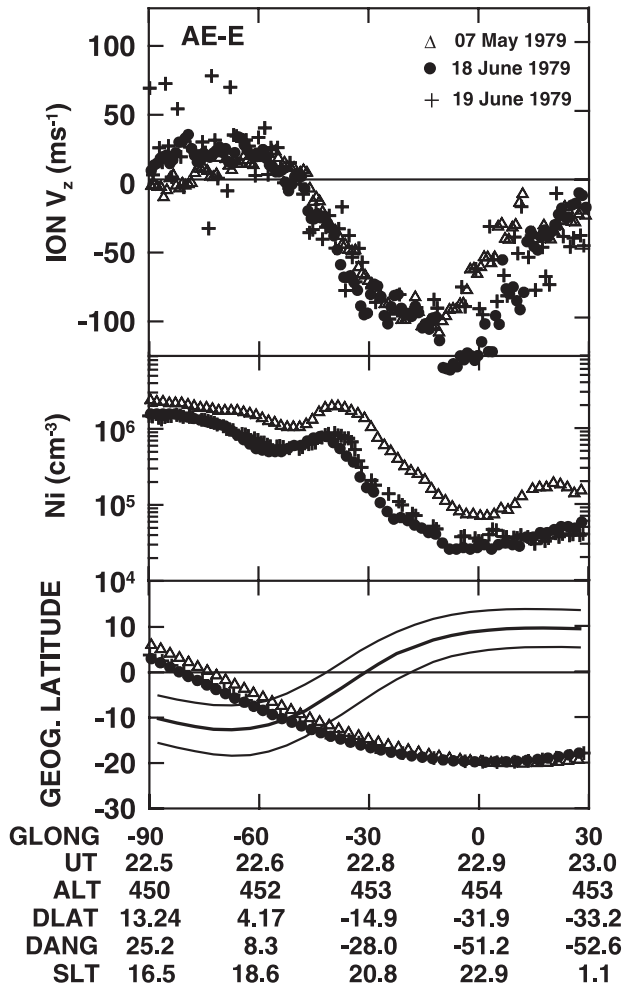

Figure 1. Measurements of (top) vertical plasma drift velocity and (middle) plasma density along the AE-E satellite trajectory during June solstice at solar maximum. (bottom) The AE-E trajectories and the locations of the dip equator and of the 5° dip latitude contours.

Ionosphere Model (SUPIM) [*Bailey et al.*, 1993] to investigate the occurrences of these features and, also, to determine the role of the different physical processes responsible for the strong large-scale downward drifts and density depletions observed by the satellite.

2. Data

[5] The AE-E satellite had an orbital inclination of 19.76° and made low-latitude ionospheric measurements from the end of 1975 through June 1981. We have used the AE-E Ion Drift Meter (IDM) data from January 1976 through December 1979 when the satellite was in near circular orbit with altitude increasing from 250 to 470 km. The characteristics of the IDM have been described by *Hanson and Heelis* [1975]. This probe measured the ion density and the horizontal and vertical components of the ion drift velocity perpendicular to the satellite trajectory. Near the magnetic equator, the vertical drift velocity corresponds to the electrodynamic drift velocity driven by the zonal electric field, but at higher latitudes it is a combination of the drift components perpendicular and parallel to the geomagnetic field. The relative and absolute precisions of the drift measurements are ~2 and 7 m s^{-1}, respectively.

[6] The seasonal, solar cycle, and longitudinal variations of the equatorial (dip latitudes smaller than 7.5°) $\mathbf{E} \times \mathbf{B}$ drift velocity have been described by *Fejer et al.* [1995]. Recently, *Scherliess and Fejer* [1999] have presented a global empirical analytic model of the equatorial *F* region vertical drift velocity obtained from the AE-E data [*Fejer et al.*, 1995] and incoherent scatter radar measurements made at Jicamarca, Peru (11.9°S, 76.8°W; dip latitude 1°N). We have used the results of the Scherliess and Fejer model as an input parameter for the SUPIM simulations.

[7] We have examined the AE-E IDM database for June solstice and have found large downward ion drift velocities (larger than 60 m s^{-1}) and associated reductions in the ion density at a fixed altitude. These are typical features of the postsunset South Atlantic at low geographic latitudes between 350- and 450-km altitude. It should be noted that there are also large ion density gradients at a fixed altitude in the nighttime period resulting from the strong uplift of the ionosphere, as reported by *Dachev and Walker* [1982] and others, but these events will not be considered here.

[8] Figure 1 shows three examples with nighttime downward drifts exceeding 80 m s^{-1} and plasma densities smaller than 10^5 cm^{-3} at the height of the satellite (~450 km) during magnetically quiet times. These observations occurred in the 10°S–20°S and 50°W–10°E sector, which is consistent with the results of *Dachev and Walker* [1982], who used ion density and composition data from the Bennet ion mass spectrometer (BIMS) on AE-E. Figure 1 illustrates the strong longitudinal variation of the ion density and vertical ion drift resulting from the magnetic field geometry in this sector. As we will discuss later, these are permanent features of the South Atlantic low-latitude ionosphere during June solstice. In the following section, we use these observations and SUPIM to quantify the effects of the various dynamic processes responsible for these phenomena.

3. Model Results and Comparison With the Data

[9] The Sheffield University Plasmasphere Ionosphere Model (SUPIM) has been described in several papers [e.g., *Bailey and Sellek*, 1990; *Bailey et al.*, 1993; *Bailey and Balan*, 1996]. This model determines the concentrations, fluxes, and temperatures of the O^+, H^+, He^+, N_2^+, O_2^+, and NO^+ ions and electrons by solving the coupled time-dependent continuity, momentum, and energy balance equations along closed magnetic field lines. The geomagnetic field is represented by an eccentric dipole with angle of tilt and displacement of the dipole from the Earth's center determined from the 1995 International Geomagnetic Reference (IGRF) model. The concentrations and temperatures of the neutral atmospheric gases are obtained from MSIS86 [*Hedin*, 1987] and the solar EUV fluxes from the EUVAC model of *Richards et al.* [1994].

[10] Two important inputs for the model are the equatorial $\mathbf{E} \times \mathbf{B}$ vertical plasma drift and the thermospheric neutral wind in the magnetic meridian and zonal directions. In this work, we have used the empirical equatorial vertical plasma drift model developed by *Scherliess and Fejer* [1999]. The

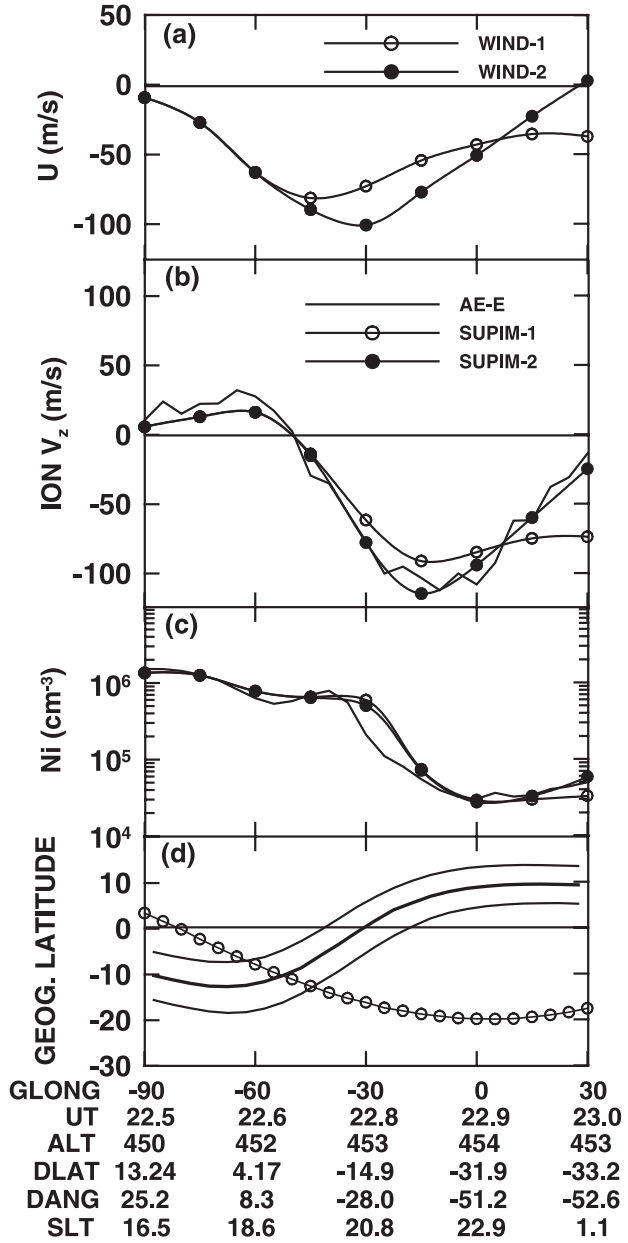

Figure 2. (a) Meridional winds from HWM90 (WIND-1) and calculated winds derived from the SUPIM calculations (WIND-2); (b) vertical plasma velocities and (c) plasma densities measured by the AE-E satellite (solid line) and calculated using Sheffield University Plasmasphere Ionosphere Model (SUPIM) with the WIND-1 and WIND-2 winds, respectively; (d) the satellite trajectory.

magnetic meridional wind (i.e., neutral wind component along the horizontal component of the geomagnetic field lines) is determined from

$$U_m = U_\theta \cos D + U_\phi \sin D, \quad (1)$$

where U_θ and U_ϕ are the geographic northward and eastward winds, respectively, and D is the magnetic declination angle [e.g., *Souza et al.*, 2000a]. The simulations with SUPIM normally use geographic winds given by the Horizontal Wind Model 1990 (HWM90) [*Hedin et al.*, 1991]. In the present work we present simulations using two meridional wind models: the standard HWM90 wind model, and a wind pattern that gives modeled vertical ion drift velocities in close agreement with the observed values.

[11] Figure 2 shows the experimental and modeled results along the satellite trajectory, which is shown in the bottom panel. Figure 2a presents the magnetic meridional winds derived from equation (1) using HWM90 (WIND-1) and the adjusted wind model (WIND-2). These winds have maximum southward values of around 80 and 100 m s^{-1} near 45°W and 30°W, respectively. Figures 2b and 2c present the measured and calculated vertical ion drift velocities and ion densities along the satellite trajectory using the meridional wind patterns displayed in the top panel. The vertical ion drift velocities result from the combined effects of the electrodynamic plasma drift, magnetic meridional neutral wind and diffusion. The model results of Figure 2d are in excellent agreement with the measured satellite ion densities.

[12] We have also used the modeled values to quantify the effects of the winds in the magnetic meridian, **E** × **B** drift, and diffusion on the vertical ion drift velocity. Diffusion results from the effects of gravity, pressure gradients, and collisions between the ion and neutral gases. Figure 3 shows the contributions of **E** × **B** drift, neutral wind, and diffusion to the vertical ion drift computed along the satellite track. The variations show longitudinal, latitudinal and local time effects. Near the equator the **E** × **B** drift undergoes a reversal from upward to downward associated with passage across sunset. Between 60°W and 30°W the zonal wind contributes greatly to the magnetic meridional component, while the satellite motion to higher dip latitudes allows this component to increasingly contribute to the vertical ion drift. Most important is the role that the wind plays in lowering the *F* peak after sunset, resulting in rapid recombination and associated downward diffusion of the

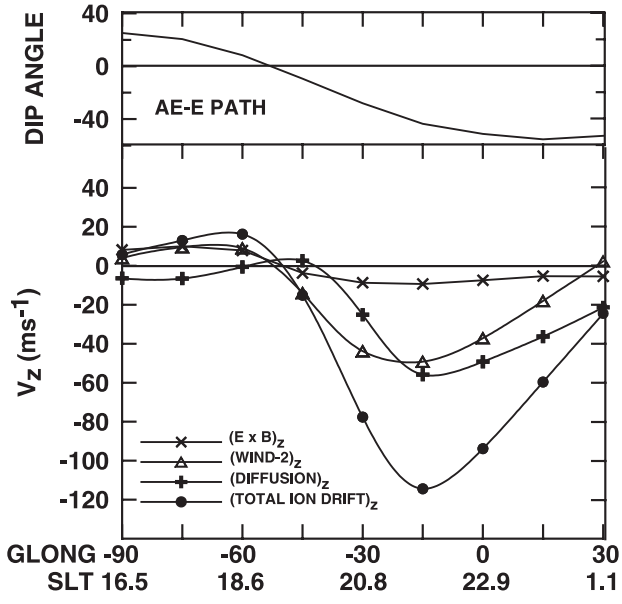

Figure 3. (bottom) Vertical ion drift velocities along the (top) satellite track.

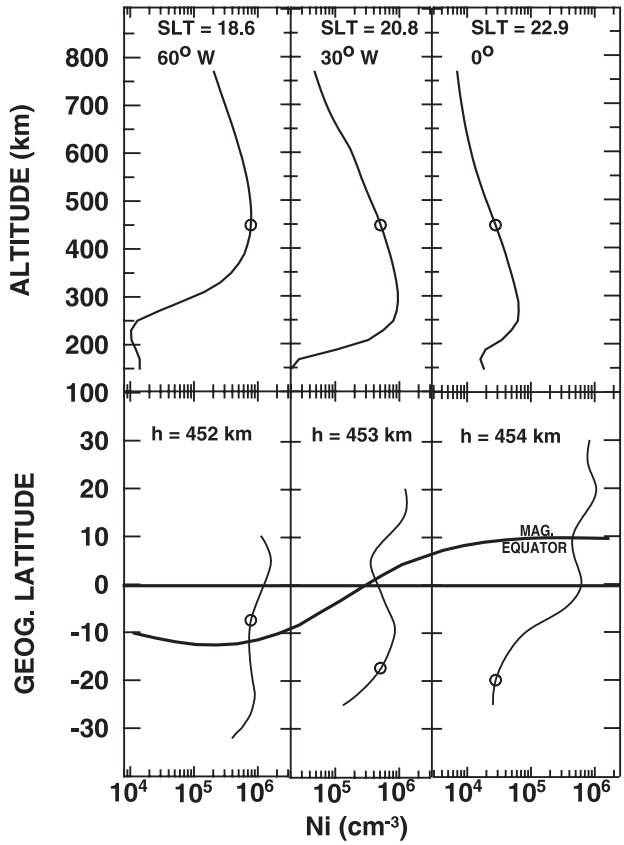

Figure 4. (top) Altitudinal and (bottom) latitudinal ion density profiles calculated using SUPIM. The open circles show the heights and latitudes of the AE-E satellite at longitudes 60°W, 30°W, and 0°.

ions. In fact, we see that the downward diffusion accounts for ~50% of the inferred vertical ion drift.

[13] To first order, the variation of the ion density along the satellite path shown in Figure 2 corresponds to a typical day-night transition, i.e., high ion densities in the topside during the day and smaller topside densities at night. However, the observed ion densities along the satellite track can only be understood by taking into account the passage of the satellite through regions where longitudinal, latitudinal, and local time gradients exist. The bottom panel in Figure 4 shows latitudinal ion density profiles calculated with SUPIM at the height of the satellite (about 450 km) at longitudes of 60°W, 30°W, and 0° at local times corresponding to those at which the satellite crosses these longitudes. The top panel presents the corresponding altitude profiles at the latitude of the satellite. The latitudinal ion density profiles show Appleton anomaly peaks past local sunset and, as expected, larger ion density peaks to the north, as a result of the southward thermospheric wind. At 60°W the satellite was inside the anomaly trough, but the ion density was high since this crossing occurred near sunset close to the *F* layer peak. At 30°W the satellite crossing occurred south of the southern anomaly peak at about 150 km above the *F* layer peak. As shown in Figure 2, the calculated ion density is larger than the observed value. At 0° the *F* peak height is lower due to the action of magnetic meridional wind after sunset. The satellite crossing altitude is about 200 km above the peak, where the density is significantly lower than observed at previous locations.

[14] The AE-E measurements show smaller gradients in the density along the satellite track in the absence of large postsunset downward ion velocities during equinox and December solstice. Such behavior is also seen in the SUPIM results (see Figure 5). This is to be expected since the magnetic meridional wind is northward for December and weakly southward during equinox, resulting in smaller nighttime downward drift velocities. On the other hand, noticable ion density reductions at fixed altitude are observed as a function of longitude in the North Atlantic region during December solstice as pointed out by *Dachev and Walker* [1982]. However, the magnitudes of these

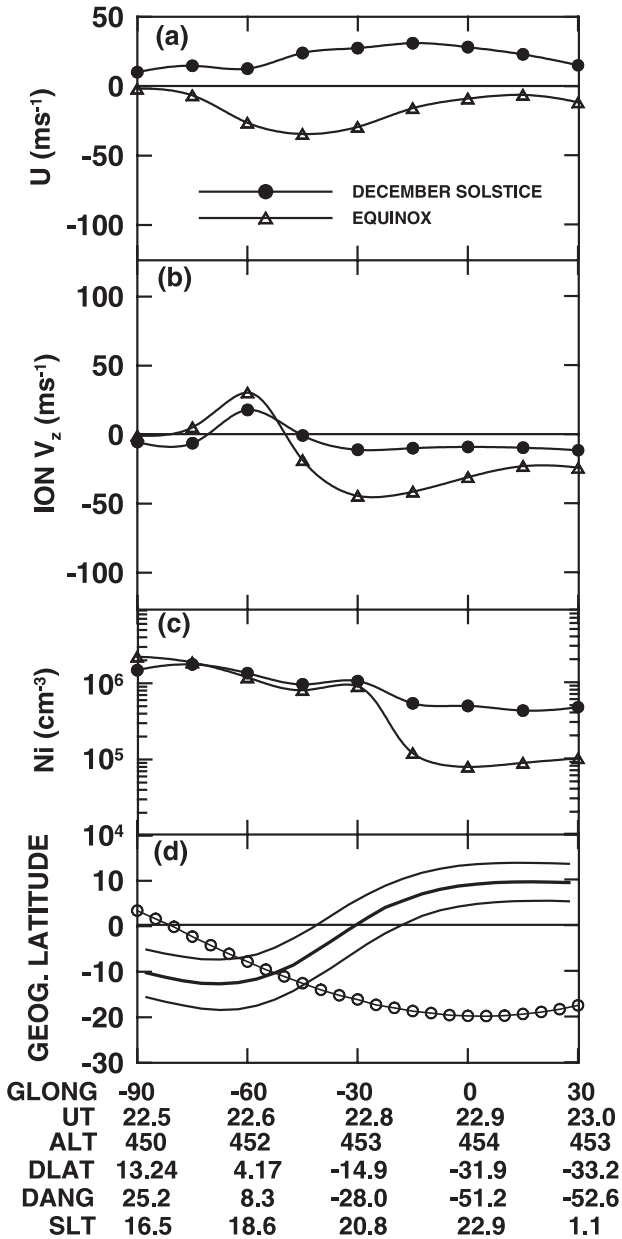

Figure 5. Same as Figure 2, but for equinox and December solstice. WIND-1 is used in the SUPIM and satellite data are not presented.

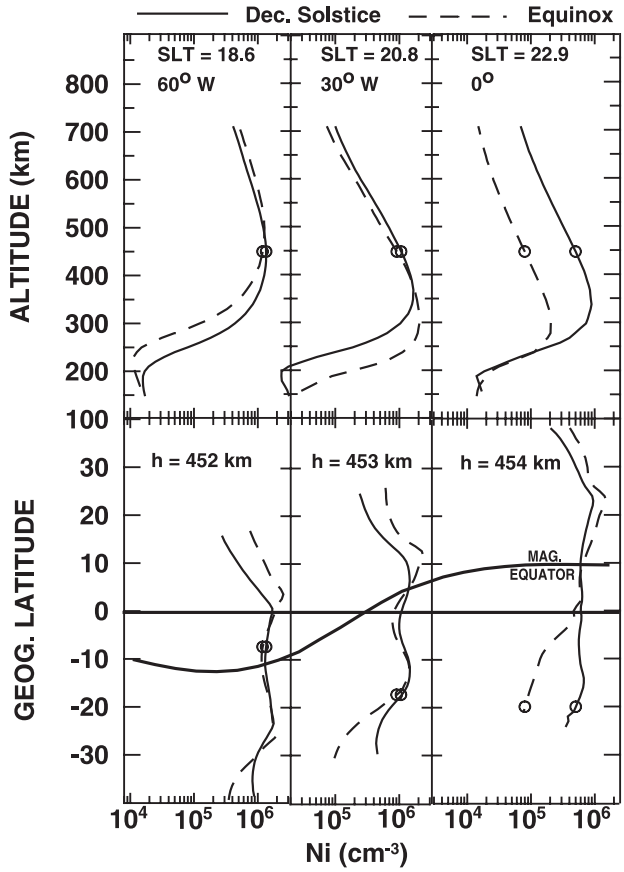

Figure 6. Same as Figure 4, but for equinox and December solstice.

downward drift velocities and density depletions are smaller than presented above for June solstice since, in this Northern Hemisphere sector, the evening eastward wind gives an upward ion drift component. Figure 6 shows, in clear way, the role played by the $\mathbf{E} \times \mathbf{B}$ drift and winds to control the variation of ion density with the altitude (top panel), latitude (bottom panel) and longitude for equinox and December solstice. Considering the same satellite altitude and trajectory of June solstice, it is found that near the magnetic equator in both equinox and December solstice the vertical distribution is controlled by $\mathbf{E} \times \mathbf{B}$ drift (first block). This is also noticed in June solstice. In equinox, near the southern anomaly crest (middle block) from the altitude profile of ion density for 20.8 SLT, we can see a definite increase in ion density up to an altitude of ~350 km, as compared to December solstice. This is due the fact that after prereversal enhancement of the $\mathbf{E} \times \mathbf{B}$ drift diffusion and meridional magnetic wind in southward direction move the plasma down increasing the ion density in lower altitude for few hours. This will subsequently be destroyed by recombination, as we can see by comparing the latitudinal profiles in block two and three. In general, outside the Appleton anomaly, the equinox (December solstice) winds in southward (northward) direction move up (down) the ionospheric layers decreasing (increasing) the recombination, consequently the F-region density increases (decreases) in north hemisphere while the reverse occur in South Hemisphere as showed in lower panels of Figure 6.

[15] During equinox and December solstice a decrease of the late afternoon total electron content (TEC) and *F* region critical frequency, followed by a postsunset enhancement are well known features of the American-African sector [*Anderson and Klobuchar*, 1983; *de Paula et al.*, 1996]. SUPIM results (Figure 5c) have not shown clear manifestation of these features since the satellite trajectory is slightly outside the crest of Appleton Anomaly and above the *F* region ionization peak. However, from the height profiles of ion density in Figure 6, particularly in equinox, an increase in N_{max} at 20.8 SLT compared to 18.6 SLT is evident.

4. Summary

[16] We have presented early nighttime AE-E satellite measurements of large gradients in the ion density and vertical ion drift as a function of longitude at nearly fixed altitude and geographic latitude in the South American sector. These large perturbations occur during June solstice and result in large ionospheric longitudinal variations. The large downward ion drift velocity is due to combined effects of diffusion and the zonal and meridional neutral winds.

[17] Using the SUPIM model we find that the geographic north-south and east-west winds combine to maximize the magnetic meridional component in this region of maximum negative declination. After sunset these winds act to lower the *F* peak and increase the recombination rate between the ions and neutral gases. This results in the largest observed downward ion drifts. These calculations confirm that the large gradients in ion density and downward ion drift observed by the AE-E satellite are consistent with the passage of the satellite from day to night into a region where the magnetic meridional wind component and the dip latitude are increasing.

[18] **Acknowledgments.** The work at INPE was supported by FAPESP-Fundacão de Amparo a Pesquisa no Estado de São Paulo, under contracts 92/01267-2, 98/02010-1, 99/00437-0, 00/12735-5 and by CNPq-Conselho Nacional de Desenvolvimento Científico e Tecnológico, Brazil, under process 201239/87-6, at Utah State University by the National Aeronautics and Space Administration through grants NAGW-4469 and NAGS-10215 , and by the Aeronomy Program of the Nacional Science Foundation through grant ATM-0004380, and that at the University of Sheffield by the Particle Physics and Astronomy Research Council (PPARC, UK) under grant PPA/G/O/1999/00568.

References

Abdu, M. A., J. H. A. Sobral, I. S. Batista, V. H. Rios, and C. Medina, Equatorial spread-*F* occurrence statistics in the American sector: Diurnal, seasonal, and solar cycle variations, *Adv. Space Res.*, *22*(6), 851–854, 1998.

Anderson, D. N., A theoretical study of the ionospheric *F*-region equatorial anomaly, II, Results in the American and Asian sectors, *Planet. Space Sci.*, *21*, 421–442, 1973.

Anderson, D. N., and J. A. Klobuchar, Modeling the total electron content observations above Ascencion Island, *J. Geophys. Res.*, *88*, 8020–8024, 1983.

Bailey, G. J., and N. Balan, A low-latitude ionosphere-plasmasphere model, in *STEP Handbook on Ionospheric Models*, edited by R. W. Schunk, pp. 173–206, Utah State Univ., Logan, 1996.

Bailey, G. J., and R. Sellek, A Mathematical model of the Earth's plasmasphere and its application in a study of He at *L*=3, *Ann. Geophys.*, *8*, 171–190, 1990.

Bailey, G. J., R. Sellek, and Y. Rippeth, A modeling study of the equatorial topside ionosphere, *Ann. Geophys.*, *11*, 263–272, 1993.

Batista, I. S., M. A. Abdu, and J. A. Bittencourt, Equatorial *F*-region vertical plasma drifts: Seasonal and longitudinal asymmetries in the American sector, *J. Geophys. Res.*, *91*, 12,055–12,064, 1986.

Basu, Su., S. Basu, C. E. Valladares, H.-C. Yeh, S.-Y. Su, E. MacKenzie, P. J. Sultan, F. J. Rich, P. Douherty, K. M. Groves, and T. W. Bullet, Ionospheric effects of major magnetic storms during the pace weather period of September–October 1999: GPS observations, VHF/UHF scintillations and in situ density structures at middle and equatorial latitudes, *J. Geophys. Res.*, *106*, 30,389–30,413, 2001.

Dachev, T. P., and J. C. G. Walker, Seasonal dependence of the distribution of large-scale plasma depletions in the low latitude *F* region, *J. Geophys. Res.*, *87*, 7625–7639, 1982.

de Paula, E. R., J. R. de Souza, M. A. Abdu, G. J. Bailey, I. S. Batista, J. A. Bittencourt, and E. Bonelli, Ionospheric electron content over Brazilian low latitude and its comparison with the IRI and SUPIM model, *Adv. Space Res.*, *18*(6), 245–248, 1996.

Fejer, B. G., E. R. de Paula, S. A. Gonzalez, and R. F. Woodman, Average vertical and zonal *F*-region plasma drifts over Jicamarca, *J. Geophys. Res.*, *96*, 13,901–13,906, 1991.

Fejer, B. G., W. B. Hanson, and R. A. Heelis, Satellite observations of low latitude ionospheric plasma depletions, in *Proceedings of the COSPAR Colloquium on Low-Latitude Ionospheric Physics*, edited by F.-S. Kuo, pp. 51–56, Pergamon, New York, 1993.

Fejer, B. G., E. R. de Paula, R. A. Heelis, and W. B. Hanson, Global equatorial ionospheric plasma drifts measured by the AE-E satellite, *J. Geophys. Res.*, *100*, 5769–5776, 1995.

Hanson, W. B., and R. A. Heelis, Techniques for measuring bulk gas motions from satellites, *Space Sci. Instrum.*, *1*, 493, 1975.

Hedin, A. E., MSIS-86 thermospheric model, *J. Geophys. Res.*, *92*, 4649–4662, 1987.

Hedin, A. E., et al., Revised global model of upper thermosphere winds using satellite and ground-based observations, *J. Geophys. Res.*, *96*, 7657–7688, 1991.

Richards, P. G., J. A. Fennely, and D. G. Torr, EUVAC: A solar EUV flux model for aeronomic calculations, *J. Geophys. Res.*, *99*, 8981–8992, 1994.

Scherliess, L., and B. G. Fejer, Radar and satellite global equatorial vertical drift model, *J. Geophys. Res.*, *104*, 6829–6842, 1999.

Souza, J. R., G. J. Bailey, M. A. Abdu, and I. S. Batista, Ionospheric modeling at low latitudes over Brazil during summer solar maximum, *Adv. Space Res.*, *25*(1), 133–138, 2000a.

Souza, J. R., M. A. Abdu, I. S. Batista, and G. J. Bailey, Determination of vertical plasma drift and meridional wind using the Sheffield University Plasmasphere Ionosphere Model and ionospheric data at equatorial and low latitudes in Brazil: Summer solar minimum and maximum conditions, *J. Geophys. Res.*, *105*, 12,813–12,821, 2000b.

Sultan, P. J., F. J. Rich, W. J. Burke, and C. Y. Huang, Topside ionospheric response to large geomagnetic disturbances (abstract), *Eos Trans. AGU*, *82*(20), Spring Meet. Suppl., S290, 2001.

Venkatraman, S., and R. A. Heelis, Longitudinal and seasonal variations in nighttime plasma temperatures in the equatorial topside ionosphere during solar maximum, *J. Geophys. Res.*, *104*, 2603–2611, 1999.

G. J. Bailey, Department of Applied Mathematics, University of Sheffield, S3 7RH Sheffield, England, UK.

E. R. de Paula and J. R. Souza, Instituto Nacional de Pesquisas Espaciais, São José dos Campos, São Paulo, Brazil.

B. G. Fejer, Center for Atmospheric and Space Sciences, Utah State University, Logan, UT 84222-4405, USA.

R. A. Heelis, W. B. Hanson Center for Space Sciences, University of Texas at Dallas, Richardson, TX 75083-0688, USA.